Fabrication and Characterization of Potassium and Sodium Titanate via a Hydrothermal Method

[1] Jiasheng Xu [*], [1] He Zhang, [2] Tongchao Liu and [1] Jie Zhang
[1]*Liaoning Province Key Laboratory for Synthesis and Application of Functional Compounds, College of Chemistry, Chemical Engineering and Food Safety, Center of Science and Technology Experiment, Bohai University, 19 Sci-tech Road, Jinzhou 121013, P.R. China.*
[2]*College of Chemical and Environmental Engineering, Qingdao University, Qingdao, 266071, P R China.*
jiashengxu@bhu.edu.cn*

(Received on 12th April 2013, accepted in revised form 14th October 2013)

Summary: Various sized titanate nanofibers were prepared by hydrothermal reaction of aqueous solutions containing the respective alkali (KOH and NaOH) and anatase in stoichiometric amounts at 170-200 °C for 96 h. Their morphological and structural properties were characterized by many methods, including the powder X-ray diffraction (XRD), the scanning electron microscopy (SEM), the fourier transform infrared spectroscopy (FTIR) and the UV/Vis spectrophotometer. Their morphologies depend on the experimental temperature and the solution conditions, in which the alkali metal plays an important role during the experimental process. When the size of titanate samples decrease, the UV-Vis spectra are blue-shift. This work provided an effective hydrothermal method to synthesize titanate nanofibers, which may be applicable to fabrication of other nanomaterials.

Keywords: Titanate, Nanofibers, Hydrothermal, X-Ray Diffraction, Temperature.

Introduction

Recently, morphology-controlled fabrication of inorganic materials on a nanometer scale has achieved much progress. Understanding the morphology-structure and function relationship is very important for further fabricating highly functional materials in the practical applications [1-8]. Among the several attractive materials studied so far, titanate exhibits many morphologies ranging from fibers, tubes, wires, belts, rods, rings and so on[9-17]. Alkaline metal titanates with different structures have been investigated intensively due to their unique ferroelectric, dielectric, and piezoelectric properties. These properties are very important in the technological applications such as photocatalysis, solar energy conversion, semiconductors, photovoltaic devices, self-cleaning devices, gas sensors, selective adsorption, ion exchange, lithium-ion-battery, ultraviolet blockers and smart surface coatings [18-31].

The hydrothermal method has been successfully used to fabricate nanotubes of TiO_2-related materials without using any other templates [17, 32]. Many investigations have been conducted on the fibers grown in the NaOH solution [33]. The titania nanotubes with a diameter less than 10 nm could be synthesized by a reaction of NaOH and TiO_2 nanoparticles (anatase or rutile structure). The obtained nanotubes can be built in a layered titanate structure trititanate of the composition $M_2Ti_3O_7$ or $M_xH_{2-x}Ti_3O_7$ (M= Na or K) [34]. Furthermore, these techniques may be applied for the fabrication of titanate nanowires using KOH (a.q.) [35]. However the formation, structure, morphology, and properties of titanates are not yet completely understood.

Herein, we prepare potassium and sodium titanate nanofibers by reacting concentrated KOH and NaOH solution with TiO_2 anatase powders via a one-step hydrothermal reaction. It is found that the reaction temperature and reaction solution are important for the morphology of titanate. The composition of the as-prepared titanate nanostructure has been investigated. All the chemical reagents used in this work are commercially available. Meanwhile, it has a potential value to fabricate the other inorganic nanomaterials through this simple, environmentally acceptable, and economic method.

Results and Discussion

Table-1: A collection of experimental conditions.

No.	KOH (mol)	NaOH (mol)	*T* (°C)	Result
1	0	0.3	170	Fig.1A; Fig.3A; Fig.5A; Fig.7A
2	0	0.3	180	Fig.1B; Fig.3B; Fig.5B; Fig.7B
3	0	0.3	190	Fig.1C; Fig.3C; Fig.5C; Fig.7C
4	0	0.3	200	Fig.1D; Fig.3D; Fig.5D; Fig.7D
5	0.3	0	170	Fig.2A; Fig.4A; Fig.6A; Fig.8A
6	0.3	0	180	Fig.2B; Fig.4B; Fig.6B; Fig.8B
7	0.3	0	190	Fig.2C; Fig.4C; Fig.6C; Fig.8C
8	0.3	0	200	Fig.2D; Fig.4D; Fig.6D; Fig.8D

[*]**To whom all correspondence should be addressed.**

The XRD patterns of as-prepared sodium titanate are shown in Fig. 1. It can be seen that the crystal phase of the as-prepared sodium titanate nanofibers depends on the experimental temperature. The alkali metal plays an essential role during the hydrothermal process. All the peaks in these XRD patterns of the product formed at different temperature may be identical to the same material. The strong diffraction peaks of $2\theta \approx 9.78°$, 27.85°, and 33.38° may correspond with the (200) plane, (310) plane and (301) plane of $H_2Ti_2O_5 \cdot H_2O$ (JCPDS No. 47-0124). The other strong diffraction peaks of $2\theta \approx 10.22°$, 16.40° and 28.96° may correspond with the (011), (111), and (220) plane of $H_2Ti_4O_9 \cdot H_2O$ (JCPDS No. 36-0655). The layer structure of $Na_2Ti_2O_5 \cdot H_2O$ and $Na_2Ti_4O_9 \cdot H_2O$ are similar to $H_2Ti_2O_5 \cdot H_2O$ and $H_2Ti_4O_9 \cdot H_2O$. Meanwhile, the diffraction peaks of 9.78°, 27.85°, and 33.38° may be supposed to correspond with (200), (310), and (301) plane of $Na_2Ti_2O_5 \cdot H_2O$. The diffraction peaks of 10.22°, 16.40°, and 28.96° may be supposed to correspond with the (011), (111), (220) plane of $Na_2Ti_4O_9 \cdot H_2O$ [36].

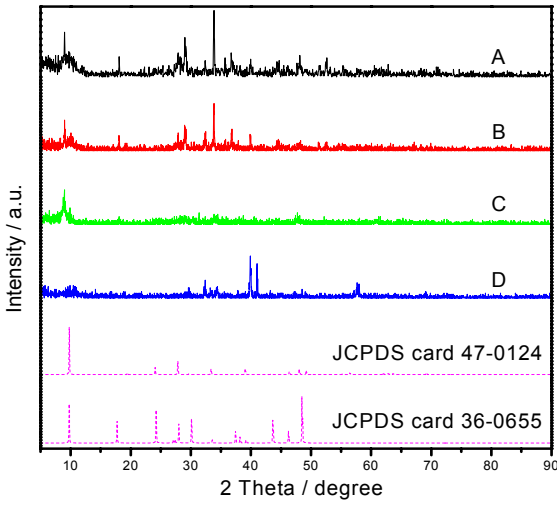

Fig 1: The typical XRD patterns of titanate synthesized by treating anatase with 10 M NaOH for 96 h at A) 170 °C; B) 180 °C; C) 190 °C; D) 200 °C. The experimental conditions are given in Table-1. The solid curves are the experimental XRD patterns; the dashed curve is the simulated patterns, which are carried out with the data JCPDS No. 47-0124 ($H_2Ti_2O_5 \cdot H_2O$) and JCPDS No. 36-0655 ($H_2Ti_4O_9 \cdot H_2O$).

From the samples *A* to *D* in Fig. 1, the three peaks ($2\theta \approx 10$ °, 28°, and 33°) become weak with the increase of experimental temperature. The crystallinity of the materials is gradually decreased, when the experimental temperature is gradually increased. With an increase in the temperature, the diffraction peaks ($2\theta \approx 10°$) become weak. From the above analysis, all the peaks may not be clearly indexed as a pure phase of titanate. The as-prepared products may be a mixture phase of $Na_2Ti_2O_5 \cdot H_2O$ and $Na_2Ti_4O_9 \cdot H_2O$.

Fig. 2 shows the XRD patterns of as-prepared titanate. It can be seen that the phase of potassium titanate nanofibers strongly depends on the experimental temperature. And the alkali metal plays a key role during the hydrothermal process. The strong diffraction peaks of $2\theta \approx 24.11°$, 29.94°, and 30.13° may correspond with the (110), (31-1), and (20-3) plane of $K_2Ti_6O_{13}$ phase (JCPDS No 40-0403). The other strong diffraction peaks ($2\theta \approx 11.33°$, 12.95°, and 29.76°) correspond with the (200), (20-1) and (-311) plane of $K_2Ti_8O_{17}$ (JCPDS No 41-1100).

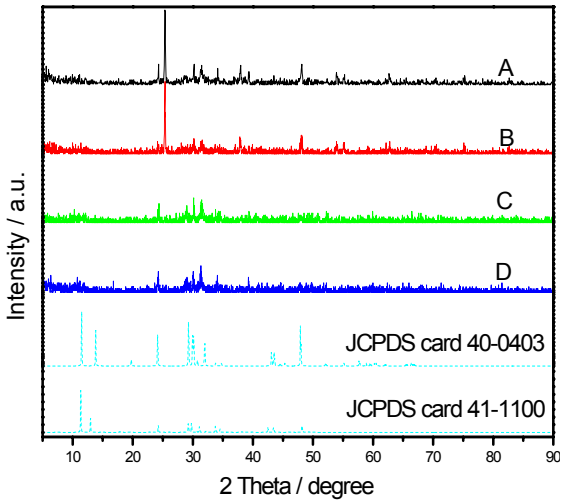

Fig 2: The typical XRD images of titanate synthesized by treating anatase with 10 M KOH for 96 h at A) 170 °C; B) 180 °C; C) 190 °C; D) 200 °C. The experimental conditions are given in Table-1. The solid curves are the experimental XRD patterns; the dashed curve is the simulated patterns, which are carried out with the data JCPDS No. 40-0403 ($K_2Ti_6O_{13}$) and JCPDS No. 41-1100 ($K_2Ti_8O_{17}$).

From the samples *A* to *D* in the Fig. 2, these

peaks ($2\theta \approx 24°$ and 30°) become gradually weak with the increase of experimental temperature. It means that the crystallinity of the product is decreased gradually, when the temperature is increased. When the temperature became high, the diffraction peak ($2\theta \approx 24°$) become weak. From the above analysis, all peaks can not be clearly indexed as a pure monoclinic phase of titanate materials (Fig. 2). The as-prepared products may be a mixture phase of $K_2Ti_6O_{13}$ and $K_2Ti_8O_{17}$.

SEM images of the titanate samples are shown in Fig. 3. It can be seen that most of the morphology are the wire-like morphology (some are aggregated). When the experimental temperature is changed, the morphologies of the titanate products are different. Therefore the experimental temperature plays a key role during this hydrothermal process.

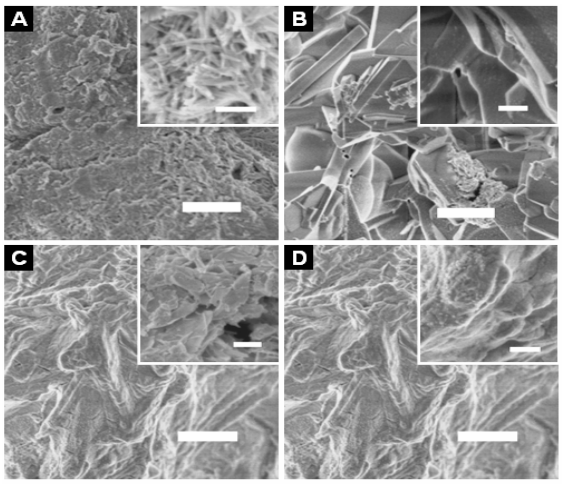

Fig. 3: The typical SEM images of as-prepared titanate synthesized by treating anatase with 10 M NaOH for 96 h at A) 170 °C; B) 180 °C; C) 190 °C; D) 200 °C. The experimental conditions are given in Table 1. The main images are Low-magnification, scale bar = 1 μm; the inserts are High-magnification, scale bar = 200 nm.

Fig. 4 shows the SEM images of the as-prepared titanate samples. It can be seen that all of the morphologies exhibit the fiber-like morphology (the ration of length/diameter is larger than 10). When the experimental temperature is changed, the morphologies of the titanate products are almost the same in the fibe-like morphology, but diameter of the fiber are different. Compared to Fig. 3, it can be clearly seen that the potassium titanate are easier to form the wire-like morphology than that of the sodium titanate during our hydrothermal process.

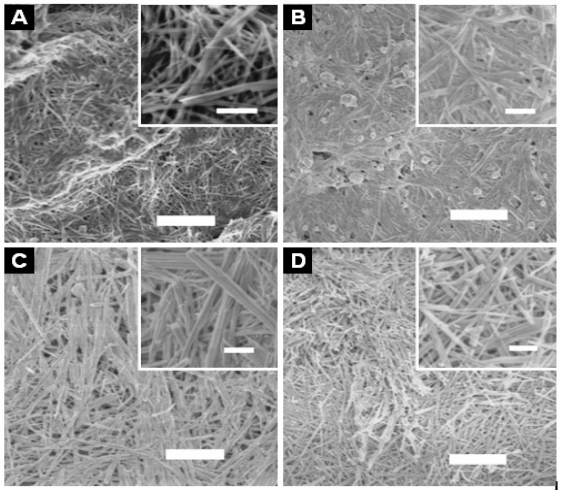

Fig. 4: The typical SEM images of as-prepared titanate synthesized by treating anatase with 10 M KOH for 96 h at A) 170 °C; B) 180 °C; C) 190 °C; D) 200 °C. The experimental conditions are given in Table-1. The main images are Low-magnification, scale bar = 1 μm; the inserts are High-magnification, scale bar = 200 nm.

In Fig. 5, the FTIR spectra peaks of the samples have a little difference. The stretching vibration peaks of –OH (~3500 cm^{-1}) are changed from sample A to D. The peak (~3500 cm^{-1}) may be attributed to O-H stretching vibrations of adsorbed water molecules or the structural -OH group. The peak (~1650 cm^{-1}) may be attributed to -OH bending vibrations. It should be pointed that the as-prepared nanofibers have the sharp absorption peaks at 470 cm^{-1}, which can be indicate the formation of trititanate structure. Moreover, the broadening of ~3500 cm^{-1} stretching vibration indicate the different -OH group. And they formed probably on Ti-OH surface. It can be seen that the -OH stretching vibration peaks (~3500 cm^{-1}) of samples (from *A* to *D*) gradually become strong with the increase of hydrothermal temperature. And the products can be a mixture phases of $Na_2Ti_2O_5 \cdot H_2O$ and $Na_2Ti_4O_9 \cdot H_2O$ (from the above XRD analysis). The stretching vibration peaks (-OH) gradually become strong due to the quantity of -OH gradually increases in the mixture phases [37, 38]

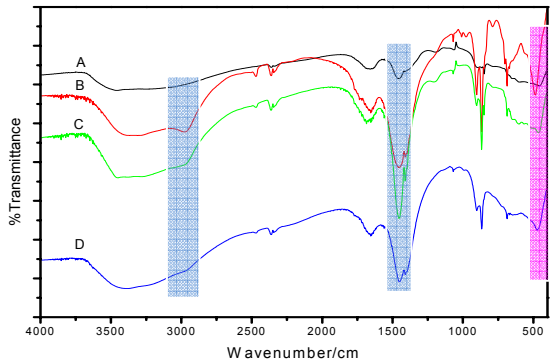

Fig. 5: FTIR spectra of as-prepared titanate synthesized by treating anatase with 10 M NaOH for 96 h at A) 170 °C; B) 180 °C; C) 190 °C; D) 200 °C. The experimental conditions are given in Table-1.

Fig. 6 shows the FTIR spectra absorption peaks of samples. The shape of the spectra is almost the same compared to Fig. 5. The peak (~3600 cm^{-1}) may be attributed to O-H stretching vibrations of adsorbed water molecules or the structural -OH groups. The peak (~1650 cm^{-1}) may be attributed to the -OH bending vibrations. It should be pointed that the as-prepared nanofibers have the sharp absorption peaks at 470 cm^{-1}, which can be indicate the formation of trititanate structure. Moreover, the -OH stretching vibration peaks of samples (from *A* to *D*) are very similar. The yield of potassium titanate has not a strong relationship with the increase of hydrothermal temperature. The samples have almost the same morphologies Fig. 4.

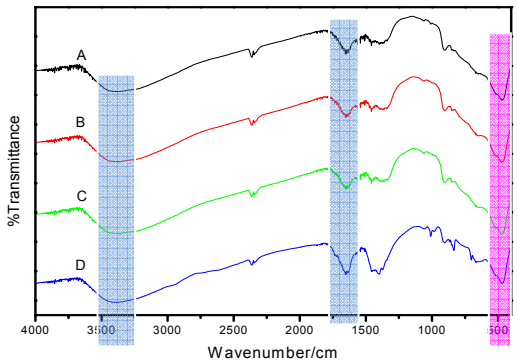

Fig. 6: FTIR spectra of as-prepared titanate synthesized by treating anatase with 10 M KOH for 96 h at A) 170 °C; B) 180 °C; C) 190 °C; D) 200 °C. The experimental conditions are given in Table-1.

Fig. 7 shows the UV vis diffuse reflectance spectra of titanate samples. The absorption properties of titanate samples changed significantly with different hydrothermal temperature. There is a blue shift for the samples from *A* to *D* compared with that of the monodispersed Titania nanosphere. The onset wavelength of the spectrum is ~370 nm in the samples *A* to *D*. The size of the titanate samples decreased, and the band-gap energies increased. Because the band-gap energy of nanoparticles increases with a decrease in the gain size [39].

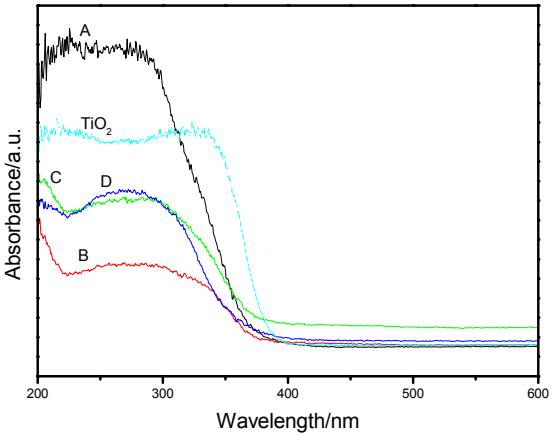

Fig. 7: UV vis diffuse spectra of the as-prepared titanate samples synthesized by treating the anatase with 10 M NaOH solution for 96 h at A) 170 °C; B) 180 °C; C) 190 °C; D) 200 °C. The experimental conditions are given in Table-1.

Fig. 8 shows the UV vis diffuse reflectance spectra of titanate samples. The absorption properties of titanate samples changed significantly. There is a blue shift in the samples *B* to *D* (except the sample *A*) compared with that of Titania sphere. The onset wavelength of the spectrum is ~370 nm in the samples *B* to *D* are about 370 nm. There is a red shift in sample *A,* compared with the Titania sphere. The onset wavelengths in the sample A are ~390 nm. In the Fig. 8, the absorption edge of the titanate samples are almost in the left side of TiO_2 (except sample *A*). In Fig. 2, there are the diffraction peaks of anatase in sample A. The sample *A* of the UV/Vis spectra is similar with the TiO_2, which may prove indirectly that the sample *A* contained more TiO_2 as a mixture phase.

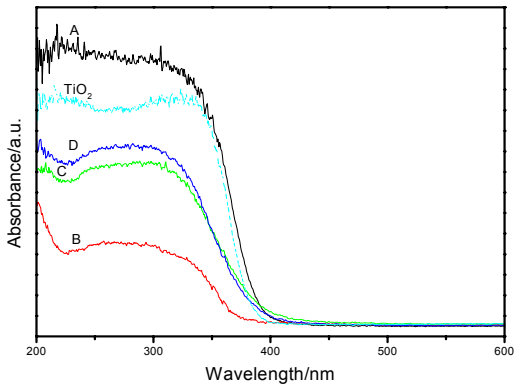

Fig. 8: UV vis diffuse spectra of the as-prepared titanate samples synthesized by treating the anatase with 10 M KOH solution for 96 h at A) 170 °C; B) 180 °C; C) 190 °C; D) 200 °C. The experimental conditions are given in Table-1.

Experimental

In is work, all of the chemical reagents were analytical grade. The samples are synthesized from anatase powder using a simple hydrothermal approach in the different alkaline solution, which is similar to the method reported in our previous work [40, 41]. The anatase powder was mixed with the concentrated KOH or NaOH solution, and then ultrasonicated for 10~20 min. Then the mixed solution was transferred into the Teflon-lined stainless steel autoclave. Then the autoclave was maintained for 96 h at the temperature of 170 °C, 180 °C 190 °C and 200 °C in an electric oven. Then, the autoclave was cooled down naturally to room temperature. And the obtained white precipitates were filtered and washed with deionized water. Finally, the as-prepared samples were dried at 50 °C for 5 h. The detail experimental conditions are given in Table-1.

The phases and structure of the as-prepared titanate samples were further characterized by powder X-ray diffraction (XRD, D/Max 2400, Rigaku, by a diffractometer) in the 2θ angles ranging from 5º to 90º. The FT-IR spectra were recorded on a Fourier transform infrared spectrometry (FT-IR, KBr disk method; NEXUS) at wavenumbers in the range 450-4000 cm^{-1}. The morphology and size of titanate samples were characterized by a scanning electron microscope (SEM, JSM-5600LV). The UV/vis diffuse reflectance spectra were recorded on a UV-vis-NIR spectrophotometer (JASCO. V-550).

Conclusion

In this work, the morphologies of the as-prepared titanate strongly depend on the experimental conditions. In the hydrothermal process, the alkali metal plays a key role. It can be demonstrated that the titanate samples exhibit a sharp optical absorption peak, and the blue-shifted relative to the bulk titania. This optical property is very important to ensure their properties performance in the various applications. We have provided a simple and effective approach to synthesize titanate nanofibers in the alkali solution (NaOH or KOH).

References

1. Z. Xiong and X. Zhao, *Journal of the American Chemical Society*, **134**, 5754 (2012).
2. J. S. Xu and D. F. Xue, *Acta Materialia*, **55**, 2397 (2007).
3. C. L. Yan, L. J. Zou, J. S. Xu, J. S. Wu, F. Liu, C. Luo and D. F. Xue, *Powder Technology*, **183**, 2 (2008).
4. J. S. Xu, J. Zhang and J. H. Qian, *Journal of Alloys and Compounds*, **494**, 319 (2010).
5. J. Zhang, J. S. Xu, H. Zhang, X. Y. Yin, J. H. Qian, L. L. Liu, D. J. Yang and X. Y. Liu, *Micro Nano Letters*, **6**, 119 (2011).
6. D. Yang, H. Liu, Z. Zheng, Y. Yuan, J. Zhao, E. Waclawik, X. Ke and H. Zhu, *Journal of the American Chemical Society*, **131**, 17885 (2009).
7. J. Ye, W. Liu, J. Cai, S. Chen, X. Zhao, H. Zhou and L. Qi, *Journal of the American Chemical Society*, **133**, 933 (2011).
8. J. S. Xu, J. Zhang and J. H. Qian, *Materials Letters*, **64**, 771 (2010).
9. H. Zhu, X. Gao, Y. Lan, D. Song, Y. Xi and J. Zhao, *Journal of the American Chemical Society*, **126**, 8380 (2004).
10. J. Yuh, J. Nino and W. Sigmund, *Materials Letters*, **59**, 3645 (2005).
11. N. Padture and X. Wei, *Journal of the American Chemical Society*, **86**, 2215 (2003).
12. J. Urban, J. Spanier, L. Ouyang, W. Yun and H. Park, *Advanced Materials*, **15**, 423 (2003).
13. Y. Lan, X. Gao, H. Zhu, Z. Zheng, T. Yan, F. Wu, S. Ringer and D. Song, *Advanced Functional Materials*, **15**, 1310 (2005).
14. A. Kar, K. Raja and M. Misra, *Surface and Coatings Technology*, **201**, 3723 (2006).
15. N. Nuraje, K. Su, A. Haboosheh, J. Samson, E. Manning, N. Yang and H. Matsui, *Advanced Materials*, **18**, 807 (2006).
16. R. Zarate, S. Fuentes, J. Wiff, V. Fuenzalida and A. Cabrera, *Journal of Physics and Chemistry of Solids*, **68**, 628 (2007).
17. Y. Ling, J. Qi, X. Zou, X. Zhao, X. Bai and Q.

Feng, *Key Engineering Materials*, **280**, 707 (2004).
18. M. Teresa Buscaglia, C. Harnagea, M. Dapiaggi, V. Buscaglia, A. Pignolet and P. Nanni, *Chemistry of Materials*, **21**, 5058 (2009).
19. M. Wrighton, A. Ellis, P. Wolczanski, D. Morse, H. Abrahamson and D. Ginley, *Journal of the American Chemical Society*, **98**, 2774 (1976).
20. D. Bavykin, J. Friedrich and F. Walsh, *Advanced Materials*, **18**, 2807 (2006).
21. E. Leite, F. Pontes, E. Paris, C. Paskocimas, E. Lee, E. Longo, P. Pizani, J. Varela and V. Mastelaro, *Advanced Materials for Optics And Electronics*, **10**, 235 (2000).
22. H. Tokudome and M. Miyauchi, *Chemical Communications*, 958 (2004).
23. Y. Luo, I. Szafraniak, N. Zakharov, V. Nagarajan, M. Steinhart, R. Wehrspohn, J. Wendorff, R. Ramesh and M. Alexe, *Applied Physics Letters*, **83**, 440 (2003).
24. Z. Dang, T. Zhou, S. Yao, J. Yuan, J. Zha, H. Song, J. Li, Q. Chen, W. Yang and J. Bai, *Advanced Materials*, **21**, 2077 (2009).
25. D. Kang, M. Han, S. Lee and S. Song, *Journal of the European Ceramic Society*, **23**, 515 (2003).
26. P. Kim, S. Jones, P. Hotchkiss, J. Haddock, B. Kippelen, S. Marder and J. Perry, *Advanced Materials*, **19**, 1001 (2007).
27. X. Sun and Y. Li, Chemistry-*A European Journal*, **9**, 2229 (2003).
28. D. Yang, S. Sarina, H. Zhu, H. Liu, Z. Zheng, M. Xie, S. Smith and S. Komarneni, *Angewandte Chemie International Edition*, **50**, 10594 (2011).
29. C. Hsu, T. Chiu, M. Shih, W. Tsai, W. Chen and C. Lin, *The Journal of Physical Chemistry* C, **114**, 4502 (2010).
30. M. Snyder, S. Trebukhova, B. Ravdel, M. Wheeler, J. Dicarlo, C. Tripp and W. Desisto, *Journal of Power Sources*, **165**, 379 (2007).
31. Z. Tian, J. Voigt, J. Liu, B. Mckenzie and H. Xu, *Journal of the American Chemical Society*, **125**, 12384 (2003).
32. Z. Liu, D. Sun, P. Guo and J. Leckie, *Chemistry-A European Journal*, **13**, 1851 (2007).
33. M. Cortie, L. Xiao, L. Erdei, C. Kealley, A. Dowd, J. Kimpton and A. Mcdonagh, *European Journal of Inorganic Chemistry*, **2011**, 5087 (2011).
34. B. Wang, Y. Shi and D. Xue, *Journal of Solid State Chemistry*, **180**, 1028 (2007).
35. Y. Suzuki, S. Pavasupree, S. Yoshikawa and R. Kawahata, *Journal of Materials Research*, **20**, 1063 (2005).
36. C. Tsai and H. Teng, *Chemistry of Materials*, **18**, 367 (2006).
37. G. Busca, G. Ramis, J. Amores, V. Escribano and P. Piaggio, *Journal of the Chemical Society, Faraday Transactions*, **90**, 3181 (1994).
38. G. Peng, S. Chen and H. Liu, *Applied Spectroscopy*, **49**, 1646 (1995).
39. A. Alivisatos, *Science*, **271**, 933 (1996).
40. S. J. Xu, H. Zhang, J. Zhang, X. Liu, X. He, D. Xu, J. Qian, L. Liu and J. Sun, *Micro Nano Letters*, 7, 407 (2012).
41. S. J. Xu, H. Zhang, J. W. Li, Zhang, X. Liu, X. He, D. Xu, J. Qian and L. Liu, *Micro Nano Letters*, **7**, 654 (2012).